Journal of Polymer Research (2018) 25: 37
https://doi.org/10.1007/s10965-017-1431-0

ORIGINAL PAPER

pH-responsive magnetic nanocomposites based on poly(2-succinyloxyethyl methacrylate-*co*-methylmethacrylate) for anticancer doxorubicin delivery applications

Aliyeh Ghamkhari[1] · Samira Agbolaghi[2] · Nahid Poorgholy[1] · Bakhshali Massoumi[1]

Received: 18 August 2017 / Accepted: 21 December 2017 / Published online: 9 January 2018

Abstract

A novel pH-responsive Fe_3O_4/poly(2-succinyloxyethylmethacrylate-*co*-methylmethacrylate) (poly(SEMA-*co*-MMA)) nanocomposite was designed for anticancer drug delivery applications. For this propose, poly(2-hydroxyethyl methacrylate-*co*-methylmethacrylate) (poly(HEMA-*co*-MMA)) was synthesized via reversible addition-fragmentation transfer (RAFT) method. Then, poly(SEMA-*co*-MMA) was prepared by the esterification of poly(HEMA-*co*-MMA) copolymer through the reaction with an excess amount of succinic anhydride. The synthesized copolymers with acidic functional groups were adsorbed onto the surface of Fe_3O_4 nanoparticles and Fe_3O_4/poly(SEMA-*co*-MMA) nanocomposite was developed. The pH-sensitivity of Fe_3O_4/poly(SEMA-*co*-MMA) nanocomposite was confirmed via dynamic light scattering (DLS) measurements. The Doxorubicin (DOX) encapsulation efficiency was 92.6%. The release rates at pHs of 5.4 and 4 (37 °C) reached 55.7 and 62.4 wt%, respectively, and at pH = 7.4, it possessed a minimum amount around 38.3 wt% after 15 days. The synthesized nanocomposite may be find the drug delivery applications, in part thanks to their smart physicochemical properties.

Keywords RAFT · Magnetic nanocomposite · Drug delivery · pH-responsive

Introduction

The inorganic nanocomposites have been prepared in developing new properties and superior performances. It is a research realm which covers the subjects ranging from chemistry, physics, and biology to material science [1–3]. The principal applications of magnetic nanoparticles were in the biotechnology and biomedicine such as magnetic resonance imaging (MRI) [4], site-specific drug delivery [5], magnetic hyperthermia in cancer therapy [6], magnetic field-assisted extraction of cells [7], enzyme catalysis [8] and radiotherapy [9]. Nanocomposites have been mainly applied as the drug delivery systems for their large specific capacity for drug loading, strong superparamagnetism, and efficient photoluminescence. Because these particles have an ability to target a specific site like a tumor, thereby decrease the systemic distribution of cytotoxic compounds and enhance uptake at the target site [10, 11]. On other hand the pH-responsive systems have been widely used for a variety of biomedical applications [12].

Doxorubicin (DOX) has been employed widely as effective anticancer drugs. However, DOX is inappropriate as a chemotherapeutic agent, due to its short- and long-term cardiac toxicity [13, 14]. Hence, it is a task to improve the anticancer activity and reduce the systemic toxicity of DOX with development of a drug delivery system. The methyl methacrylate (MMA) is a water insoluble monomer and it has been utilized as the optoelectronic biomaterials and optic fibers, because of its good optical subsuming the high transparency and clarity as well as mechanical properties [15]. In contrast, 2-hydroxyethyl methacrylate (HEMA) is a water soluble monomer and its solubility depends on the molecular weight of poly(HEMA), which has been widely used as hydrogel and biomedical fields such as drug delivery [16].

The polymers of magnetic nanocomposites were prepared using the reversible deactivation radical polymerization or living radical polymerization [17] including

✉ Bakhshali Massoumi
bakhshalim@yahoo.com

[1] Department of Chemistry, Payame Noor University, Tehran, Iran

[2] Chemical Engineering Department, Faculty of Engineering, Azarbaijan Shahid Madani University, Tabriz, Iran

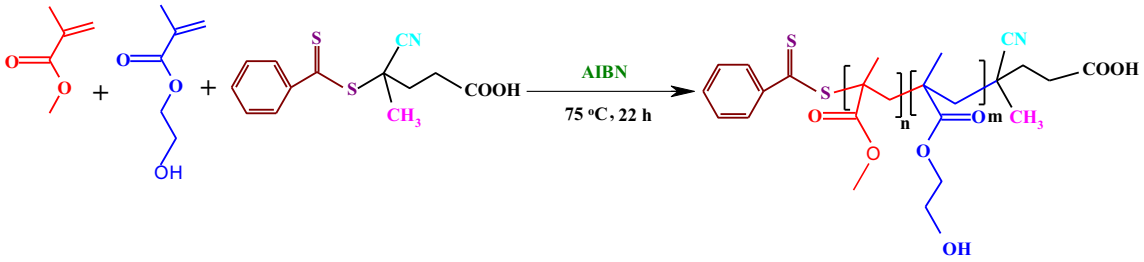

Scheme 1 Synthesis of poly(HEMA-*co*-MMA) *via* RAFT polymerization

nitroxide-mediated polymerization (NMP) [18], atom transfer radical polymerization (ATRP) [19], and reversible addition-fragmentation chain transfer (RAFT) [20]. The ATRP polymerization is limited, because the toxic catalysts cannot be removed properly from the polymers. However, due to the variety of monomers that could be polymerized in water, the RAFT polymerization is suitable for the controlled delivery, biomedical, and pharmaceutical applications [21].

The purpose of this study was the synthesis of a pH-sensitive nanocomposite as the anticancer drug delivery system. Poly(2-hydroxyethylmethacrylate-*co*-methylmethacrylate) (poly (HEMA-*co*-MMA)) was synthesized by RAFT technique. The esterification of the hydroxyl groups on poly(HEMA) blocks with excess amount of succinic anhydride resulted in poly(SEMA-*co*-MMA). These copolymers with carboxylic functional groups were then adsorbed onto the surface of Fe_3O_4 nanoparticles through the interaction with hydroxyl groups on the nanoparticles surface. The doxorubicin hydrochloride (DOX) was interacted with nanocomposite via ionic interaction and hydrogen bonding. The strong interaction of DOX with the pH-responsive blocks and pH-sensitive drug release from polymer makes the system very useful as a controlled drug delivery system [22–24].

Experimental

Materials

The RAFT agent (4-cyano-4-[(phenylcarbothioyl) sulfanyl] pentanoic acid) was synthesized in our laboratory [25]. The MMA and HEMA were distilled under reduced pressure, then were stored at −15 °C prior to use. Pyridine was dried over CaH_2. The 2,2′-azobisisobutyronitrile (AIBN), dimethyl sulfoxide (DMSO) and succinic anhydride were purchased from Sigma-Aldrich. The ferrous chloride tetrahydrate ($FeCl_2.4H_2O$, 98%), ferric chloride hexanhydrate ($FeCl_3.6H_2O$, 99%), and NH_4OH (25 wt% of ammonia) were purchased from Merck. The DOX was purchased from Zhejiang, China, and other reagents were purchased from Merck and purified according to the standard methods.

Synthesis of poly(HEMA-*co*-MMA) *via* RAFT reagent

In a typical experiment, A 200 mL three-neck round-bottom flask was loaded with MMA monomer (0.7 mL, 6.54 mmol), HEMA(0.3 mL,2.4 mmol), AIBN (1 mg, 0.005 mmol), synthesized RAFT agent (2 mg, 0.007 mmol) and dried *N*,*N*-dimethyl formamide (DMF, 5 mL). The solution was degassed with three freeze-pump-thaw cycles, and then transferred in an oil bath at 75 ± 3 °C for about 22 h. At the end of reaction time, the ampoule was transferred in cooled ice/water bath for quenching the polymerization. The mixture was precipitated in cold diethyl ether (50 mL) and, subsequently, the product was dried under vacuum at 25 °C temperature (Scheme 1).

Synthesis of poly(SEMA-*co*-MMA)

Poly(SEMA-*co*-MMA) was prepared by the esterification of poly(HEMA-*co*-MMA) copolymer through the reaction between hydroxyl groups of the poly(HEMA) with an excess

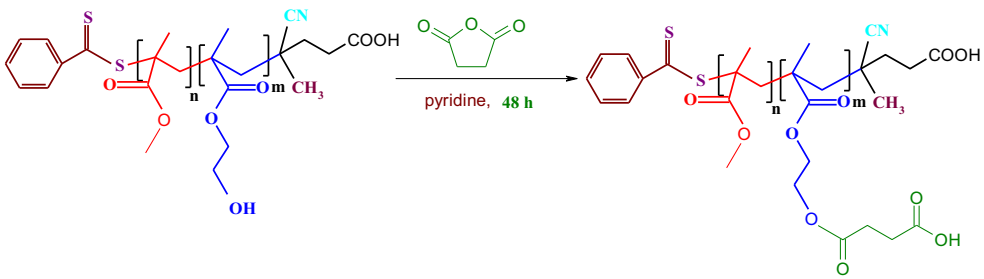

Scheme 2 Synthesis of poly(SEMA-*co*-MMA)

Fig. 1 The image of synthesized Fe_3O_4/poly(SEMA-*co*-MMA) nanocomposite in deionized water

amount of succinic anhydride. In a 150 mL round-bottom flask, poly(HEMA-*co*-MMA) copolymer (0.5 g, 0.025 mmol) was dissolved in anhydrous pyridine (20 mL) at 25 °C under the argon flow. The succinic anhydride (0.5 g, 5 mmol) was added and the reaction was proceeded at 25 °C for about 50 h. The reaction was precipitated into 50 mL of methanol to remove the excess succinic anhydride. Simultaneously, during precipitation a part of succinic anhydride was converted into monomethyl succinate which was not removed. Thus, the precipitate was re-dissolved in 15 mL of pyridine and precipitated into 150 mL of diethyl ether (Scheme 2).

Synthesis of Fe_3O_4 nanoparticles

The iron oxide nanoparticles were synthesized by coprecipitation method [26, 27]. A three-neck round-bottom flask was loaded with 200 mL of double distilled water, and then degassed by pure argon gas for 40 min. Subsequently, 20 mL of ferrous chloride (0.1 mol L^{-1}) and 40 mL of ferric chloride (0.1 mol L^{-1}) were added to the reaction. The solution was then placed in an oil bath at 80 ± 5 °C, and 10 mL of NH_4OH (25% of ammonia) was quickly added to mixture under stirring. The solution was maintained at 80 ± 5 °C for 1 h. Then, reaction was cooled and the produced black nanoparticles were washed four times with water and ethanol up to its pH became neutral. The black nanoparticles were dried under vacuum at 25 °C temperature for 24 h.

Synthesis of poly(SEMA-*co*-MMA)/Fe_3O_4 nanocomposite

The synthesized poly(SEMA-*co*-MMA) (100 mg) and Fe_3O_4 nanoparticles (100 mg) were added into a flask containing 10 mL methanol and introduced into the ultrasonic reactor. The water was circulated and then ultrasonic generator was switched on. The ampoule was irradiated with ultrasonic vibrations for 30 min to obtain a homogenous suspension. The reaction condition was similar to the preparation of nanocomposite by ultrasonic irradiation. After 30 min, the ultrasonic generator was stopped at 25 °C and the reaction was then stirred for about 30 h. After elapsing the reaction time, the unmodified iron oxide nanoparticles were precipitated by centrifugation at 8000 rpm for about 15 min and dried under vacuum at 25 °C for 24 h. In addition, the Fe_3O_4/poly(SEMA-*co*-MMA) nanocomposite was purified through an external magnetic field (Fig. 1). Four microtubes in Fig. 1 demonstrate the intermediate purification step for the nanocomposite, in which the dark areas are composed of polymer and nanoparticles.

Preparation of doxorubicin hydrochloride (DOX) -loaded magnetic nanocomposite

In this study, DOX was selected as an anticancer drug model to evaluate the drug loading. Typically, 100 mg of poly(SEMA-*co*-MMA)/Fe_3O_4 nanocomposite was ultrasonically dissolved in deionized water (15 mL) under stirring at room temperature. Then, DOX solution (10 mg) was added to the mixture and stirred for about 48 h in the dark at room temperature to reach a maximum drug loading content. The DOX-loaded magnetic nanocomposite was collected by centrifugation at 13000 rpm for 15 min. The DOX encapsulation efficiency was determined by UV-Vis spectroscopy at 480 nm and calculated using Eq. (1) [28].

$$EE(\%) = \frac{(C_T - C_{DOX})}{C_T} \times 100 \quad (1)$$

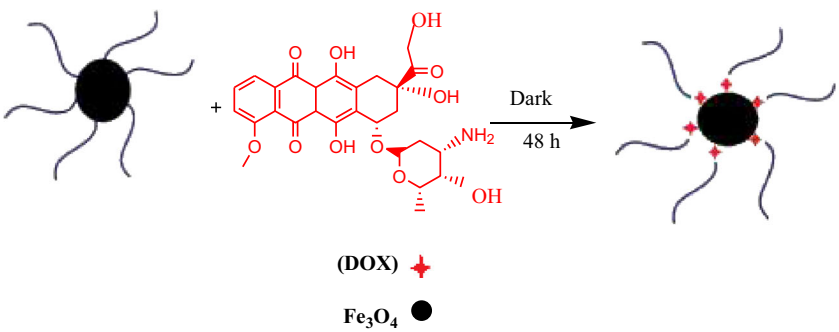

Fig. 2 The DOX loading on Fe_3O_4/poly(SEMA-*co*-MMA) magnetic nanocomposite

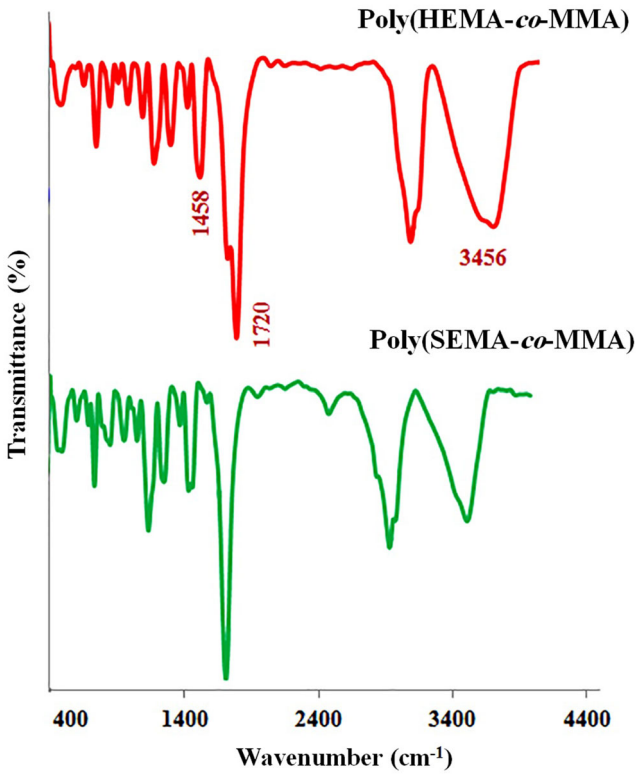

Fig. 3 FT-IR spectra of poly(HEMA-*co*-MMA) (top) and poly(SEMA-*co*-MMA) (bottom)

where C_T is total DOX concentration taken for loading and C_{DOX} is DOX concentration infiltrate solution. The DOX-encapsulation efficiency was calculated to be 94.6% and its loading efficiency was 9.3% (Fig. 2).

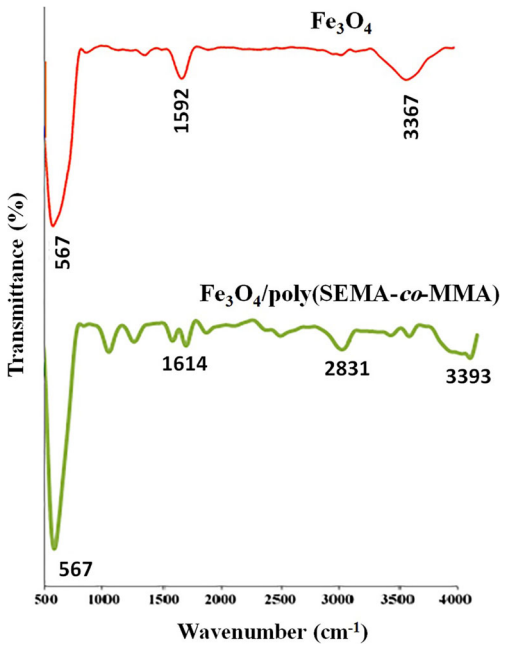

Fig. 4 FT-IR spectra of Fe_3O_4 nanoparticles (top), Fe_3O_4/poly(SEMA-*co*-MMA) magnetic nanocomposite (bottom)

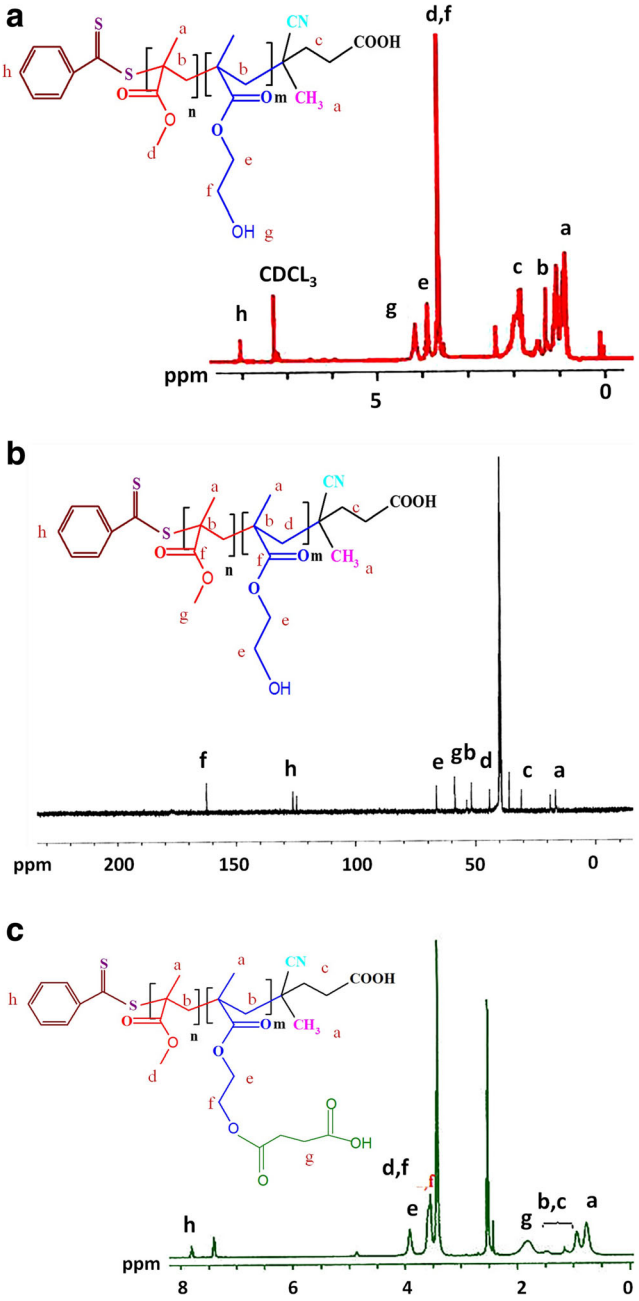

Fig. 5 ^{1}HNMR (**a** and **c**) and ^{13}CNMR (**b**) spectra of poly(HEMA-*co*-MMA) and poly(SEMA-*co*-MMA)

In vitro pH-dependent release of DOX

In the *in vitro* drug release experiment, DOX-loaded Fe_3O_4/poly(SEMA-co-MMA) magnetic nanocomposite (60 mg) was re-dispersed in buffer solution PBS (0.01 mol L^{-1},100 mL) at pHs of 7.4, 5.4, and 4, and was placed in a dialysis membrane bag with a molecular cutoff of 1 kDa. The release solution was stirred at 300 rpm at 37 °C, and then 2 mL of buffer solution was collected in different times to characterize with UV-Vis spectrophotometer at 480 nm. The percentage of the cumulative content of released DOX

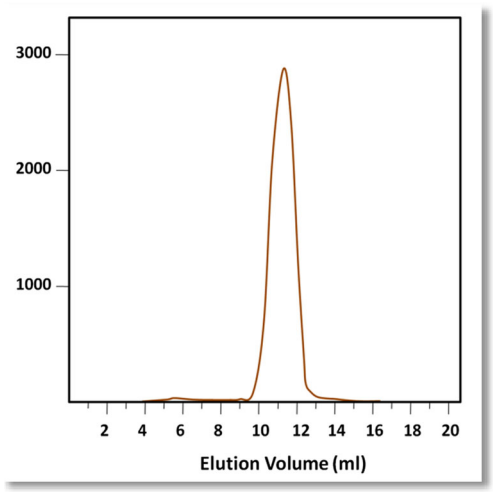

Fig. 6 GPC chromatograms of poly(HEMA-*co*-MMA) having M_n = 19,695 g/mol and M_w = 24,244 g/mol.

was deliberated from the standard calibration curve. The detected absorbance of DOX was compared with the corresponding calibration curve of DOX in the same buffer. The percent of drug released from nanocomposite was calculated based on Eq. (2) [29].

$$\textit{Cumulative released drug}\ (\%) = \frac{\textit{amount of drug in release medium at time t}}{\textit{amount loaded in nanocomposite}} \times 100 \quad (2)$$

Characterization

Fourier transforms infrared (FT-IR) spectra of the polymer and Fe_3O_4/poly(SEMA-*co*-MMA) magnetic nanocomposite were taken in a Shimadzu 8101 M FT-IR (Shimadzu, Kyoto, Japan) at 400–4000 cm^{-1}. The proton nuclear magnetic resonance (^{1}HNMR) spectra were recorded in deuterated chloroform ($CDCl_3$) at 25 °C by an FT-NMR (400 MHz) Bruker spectrometer (Bruker, Ettlingen, Germany). The size exclusion analyses were carried out using a Waters 1515 (USA) gel permeation chromatography instrument equipped with Breeze 1515 isocratic pump and 7725 manual injector. Dimethylformamide (DMF) was applied as eluent at a flow rate of 1 mL min^{-1} and column temperature of 25 °C. Magnetic properties of the Fe_3O_4/poly(SEMA-*co*-MMA) magnetic nanocomposite were evaluated by vibrating-sample magnetometer (VSM, AGFM, Iran) at 25 °C temperature. The ultraviolet-visible (UV-Vis) spectroscopic measurements were performed on a Shimadzu 1650 PC UV-Vis spectrophotometer (Shimadzu, Kyoto, Japan). The field emission scanning electron microscope (FESEM) type 1430 VP (LEO Electron Microscopy Ltd., Cambridge, UK) was applied to determine the morphologies of the synthesized samples. The structural properties were investigated by means of a X-ray powder diffraction (XRD) with a X'pert-PRO advanced diffractometer and wavelength of 1.5406 Å, and operated at 40 kV and 40 mA at room temperature in the 2θ range of 20–70°. The average diameter was measured by a laser-scattering technique (Nanotrac Wave™ (Microtrac, San Diego, CA, USA) at 25 °C. The 0.5% (*w*/*v*) solutions were prepared in deionized water, stirred for 2 h and stored for 24 h. The samples were then filtered using 0.20 μm nylon membranes (Micron Separations, Westboro, MA, USA).

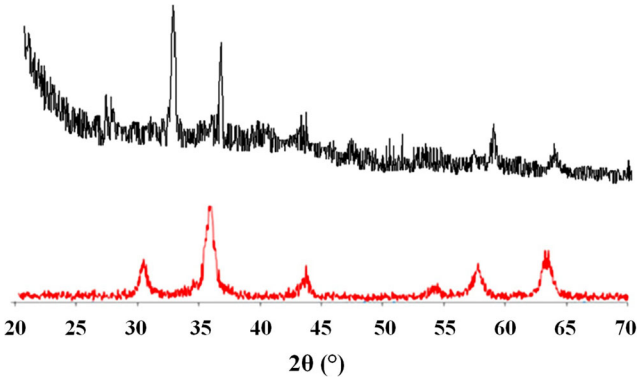

Fig. 7 X-ray diffraction patterns of Fe_3O_4/poly(SEMA-*co*-MMA) (top) nanocomposite and Fe_3O_4 nanoparticles (bottom)

Results and discussion

Magnetic nanoparticles have highly biocompatible properties; because their uptake, transport, and storage features in the liver are largely regulated by proteins such as ferritin and transferrin [30]. The aim of this study was synthesis of pH-responsive poly(SEMA-*co*-MMA)/Fe_3O_4 nanocomposite and study of its application as a nanocarrier for the anticancer drug delivery.

Characterization of poly(SEMA-*co*-MMA) copolymer

The FT-IR spectra of poly(HEMA-*co*-MMA) and poly(SEMA-*co*-MMA) are illustrated in Fig. 3. The FT-IR peaks of poly(HEMA-*co*-MMA) as followed: aliphatic C–H stretching vibrations at 2925 cm^{-1}, strong absorption band at stretching vibration of the carbonyl group at 1720 cm^{-1}, C–H bending vibration at 1458 cm^{-1}, stretching vibration of C–O group at 1375 cm^{-1} and C–O–C stretching vibration at 1255 cm^{-1}. Furthermore, the stretching vibration of hydroxyl group as a strong broad band centered at 3456 cm^{-1} (Fig. 3). After esterification of diblock copolymers with succinic anhydride, no conspicuous alteration was detected in FT-IR spectra.

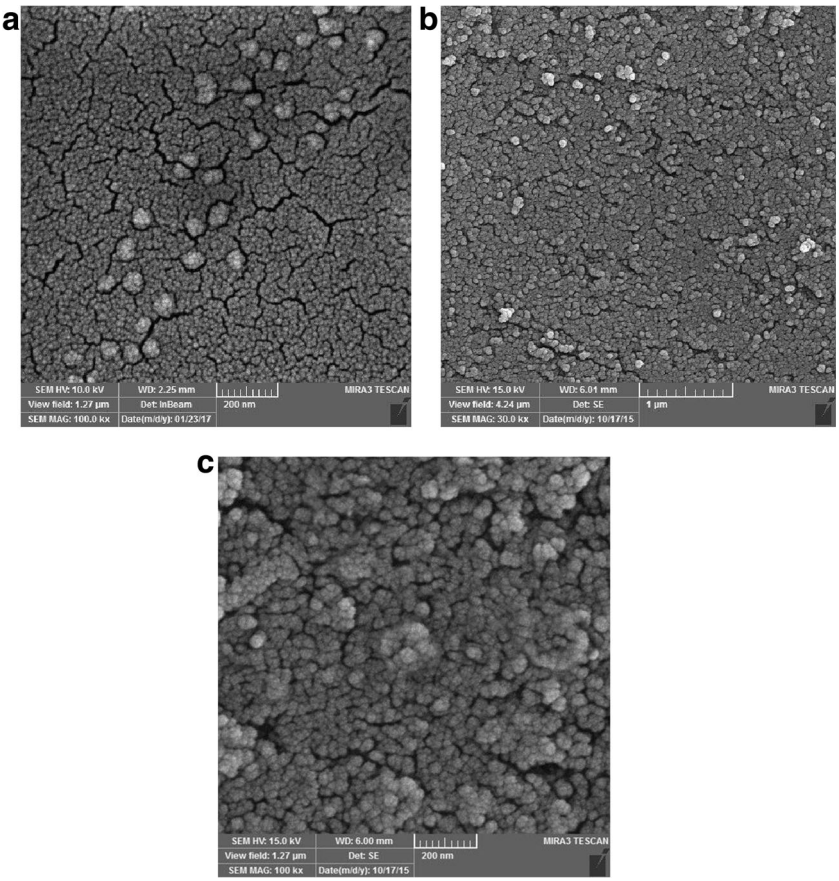

Fig. 8 FESEM image of poly(SEMA-*co*-MMA) copolymer (**a**), Fe_3O_4 nanoparticles (**b**), and Fe_3O_4/poly(SEMA-*co*-MMA) nanocomposite (**c**)

The FT-IR spectrum of Fe_3O_4 nanoparticles demonstrated the absorption bands of 567 cm^{-1} for oxygen-metal stretching vibration. The bands around 1592 and 3367 cm^{-1} were also ascribed to the bending and stretching vibrations of the hydroxyl groups on the surface of Fe_3O_4 nanoparticles, respectively. In FT-IR spectrum of the Fe_3O_4/poly(SEMA-*co*-MMA) nanocomposite, after adsorbing of polymer onto Fe_3O_4 nanoparticles, the absorption bands of C–H at 2831 cm^{-1}, carbonyl groups at 1766 cm^{-1}, C–H bending vibration at 1500 cm^{-1}, C–O–C stretching vibration at 1180 cm^{-1}, the stretching vibration of hydroxyl group as a strong broad band centered at 3393 cm^{-1} and oxygen-metal stretching vibration band at 567 cm^{-1} were detected (Fig. 4).

The synthesis of poly(HEMA-*co*-MMA) and poly(SEMA-*co*-MMA) samples were confirmed by means of ^{1}HNMR spectroscopy, as shown in Fig. 5a and b. The chemical shifts around 1.02–1.27 ppm (a) were attributed to the protons of methyl groups and the chemical shifts at 1.42–1.44 ppm (b) were associated with the methylene groups in the backbone of poly(HEMA-*co*-MMA) chain. The chemical shifts at 1.81–1.93 ppm (c) were also related to the methylene protons of RAFT backbone. The chemical shifts at 3.60 ppm were attributed to the methyl of PMMA and methylene protons of poly(HEMA) backbones (d and f), respectively. The protons of $-CH_2OH$ were observed at 3.84 ppm (e) and the chemical shift at 4.12 ppm was assigned to the hydroxyl groups of poly(HEMA). The chemical shift at 8.01 ppm (e) was also related to the aromatic protons of the RAFT agent (Fig. 5a). In addition, ^{13}CNMR spectrum of poly(HEMA-*co*-MMA) copolymers (Fig. 5b) showed the chemical shifts at 16.1–18.2 ppm ($\underline{C}H_3-C$), 30.7 ppm ($\underline{C}-CH_3$), 58.48 ppm (OCH_3) and 66.30 ppm ($O-\underline{C}H_2-\underline{C}H_2-O$), 122.47 ppm (C=C aromatic) and 162.3 ppm (CO). The successful esterification of poly(HEMA) segments into poly(SEMA) blocks was verified by the appearance of new chemical shifts at 2.22 and 2.43 ppm, relating to $-CH_2$ groups of the succinyloxy moiety. The peak of the hydroxyl group of poly(HEMA) at 4.12 ppm was disappeared, demonstrating that all of the hydroxyl groups were converted to the succinyloxy groups through the esterification (Fig. 5c). The degree of esterification (= 94.34%) was achieved by ^{1}HNMR using succinic anhydride as a judgment. The GPC chromatograms of poly(HEMA-*co*-MMA) sample is represented in Fig. 6. The polydispersity index of poly(HEMA-*co*-MMA) (PDI = 1.23) synthesized *via* RAFT polymerization was relatively low. The low dispersity suggested an excellent control over the RAFT polymerization (Fig. 6).

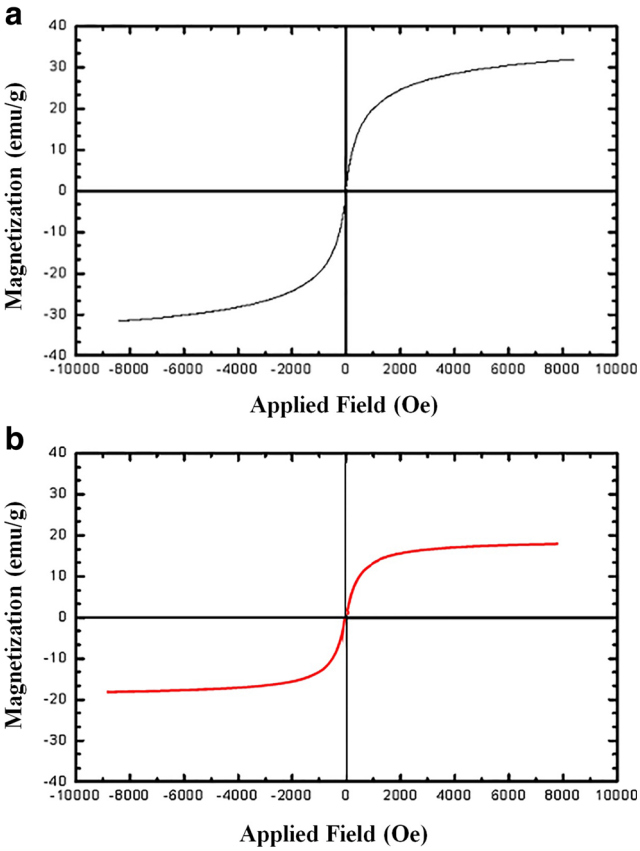

Fig. 9 Magnetization curve of Fe_3O_4 nanoparticles (**a**) and Fe_3O_4/poly(SEMA-*co*-MMA) nanocomposite (**b**)

Fig. 10 The image of the Fe_3O_4/poly(SEMA-*co*-MMA) nanocomposite in deionized water (DIW)

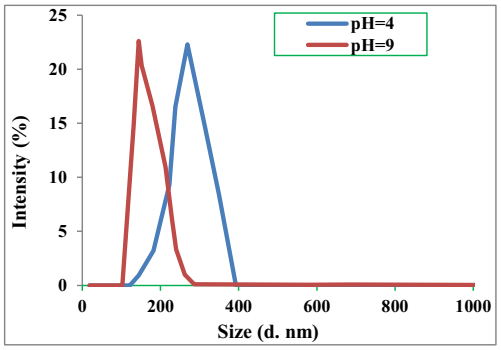

Fig. 11 DLS diagrams of Fe_3O_4/poly(SEMA-*co*-MMA) nanocomposite at pHs of 4 and 9

The X-ray diffraction study of Fe_3O_4/poly(SEMA-*co*-MMA) nanocomposite

The X-ray diffraction patterns of Fe_3O_4 nanoparticles and Fe_3O_4/poly(SEMA-*co*-MMA) nanocomposite are shown in Fig. 7. The XRD pattern for the Fe_3O_4 nanoparticles indicated distinct peaks at $2\theta = 29.6$, 35.5, 43.2, 53.1, 57.1, 62.2, and 74.2°, corresponding to the (220), (312), (400), (422), (512), (440), and (533) of Fe_3O_4 crystalline structure, respectively. The Fe_3O_4/poly(SEMA-*co*-MMA) nanocomposite also indicated similar peaks corresponding to the Fe_3O_4 nanoparticles.

Morphology and elemental composition of Fe_3O_4/poly(SEMA-*co*-MMA) magnetic nanocomposite

The FESEM images of poly(SEMA-*co*-MMA) copolymers, Fe_3O_4 nanoparticles and Fe_3O_4/poly(SEMA-*co*-MMA) nanocomposite are exhibited in Fig. 8a–c, respectively. FESEM micrograph of poly(SEMA-*co*-MMA) (Fig. 8a) showed the formation of a non-uniform surface. The Fe_3O_4 nanoparticles had spherical shapes with an average diameter of 30 ± 10 nm. The Fe_3O_4 nanoparticles had homogeneous spherical morphologies. The FESEM images demonstrated the uniformity in shape and size of prepared nanoparticles. The FESEM image of the nanocomposite (Fig. 8c) depicted that the Fe_3O_4 nanoparticles were homogeneously coordinated into the copolymer matrix through the interactions between the carboxyl and hydroxyl groups. The nanocomposite had spherical morphology with an average diameter of 40 ± 10 nm. On the basis of FESEM micrographs of Fe_3O_4/poly(SEMA-*co*-MMA) nanocomposite, there was a homogeneous dispersion of Fe_3O_4 nanoparticles in poly(SEMA-*co*-MMA) and no aggregations were detected after Fe_3O_4 nanoparticles and polymer coating.

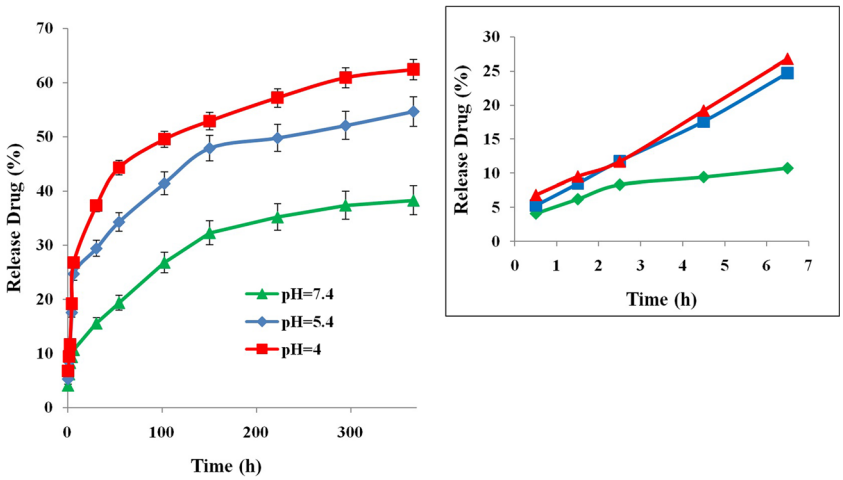

Fig. 12 *In vitro* release profiles of DOX-loaded Fe_3O_4/poly(SEMA-*co*-MMA) nanocomposites at various pHs

Magnetic properties of Fe_3O_4/poly(SEMA-*co*-MMA) nanocomposite

The VSM was a principle analysis for evaluation of nanomagnetic property. The magnetic properties of Fe_3O_4/poly(SEMA-*co*-MMA) nanocomposite were described using VSM at room temperature. As reported in Fig. 9, the saturation magnetizations (δs) of the Fe_3O_4 and Fe_3O_4/poly(SEMA-*co*-MMA) nanocomposite were around 22.23 and 13.25 $emug^{-1}$, indicating that the synthesized nanocomposite was capable of being employed in the drug delivery applications [31, 32].

Dispersibility investigation

Based on the image of Fig. 10 for Fe_3O_4/poly(SEMA-*co*-MMA) nanocomposite in deionized water, the nanocomposite was a homogeneous solution. Hence, the Fe_3O_4/poly(SEMA-*co*-MMA) nanocomposite was stabilized in deionized water as a solvent.

pH-responsivity of Fe_3O_4/poly(SEMA-*co*-MMA) nanocomposite

The pH is an important signal, which can be addressed through pH-responsive materials. The weak acids and bases such as carboxylic acids are capable of either accepting or releasing protons in response to the environmental pH changes [33]. The DLS results at pHs of 4 and 9 are illustrated in Fig. 11. The average size increased at pH = 4 and decreased at pH = 9. This is consistent with a deprotonation of poly(SEMA) at basic pH, leading to the low diameters. However, at a lower pH having a stronger repulsive interaction resulted in the larger sizes.

In vitro DOX release behavior

The use of nanoparticles as therapeutic carriers is important for their unique features like large specific quality for drug loading as well as strong magnetism. A system of magnetically targeted drug-delivery includes binding a drug to small magnetic particles, injecting these into the bloodstream, and using a high gradient magnetic field to pull them out of suspension in the target region [34, 35]. In this study, a pH-sensitive drug-delivery system consisting of DOX-loaded Fe_3O_4/poly(SEMA-*co*-MMA) nanocomposite have been successfully prepared as a drug carrier. The conjugated DOX with the magnetic nanocomposite was released in the acidic pHs. The *in vitro* DOX release behaviors of DOX-loaded Fe_3O_4/poly(SEMA-*co*-MMA) nanocomposite in different buffers, i.e., pH = 4, 5.4, and 7.4 were examined at 37 °C. As represented in Fig. 12, a quick release behavior was detected at pHs of 4 and 5.4 after 15 days. Partly at pH = 5.4 and completely at pH = 4, the protonation of carboxyl groups of nanocomposite, due to ionic interaction between DOX and nanocomposite, occurred and the release rates reached to the maximal amounts of 55.7 and 62.4 wt%, respectively (Fig. 12). The release rate in a buffer solution at pH = 7.4 reached to a minimum amount of 38.3 wt% after 15 days; because at pH of 7.4, the strong ionic interaction between DOX and nanocomposite, thanks to the deprotonation of carboxylic acids of SEMA section and protonation of DOX prohibited the drug release. At buffer with pH of 7.4, the slowest release of DOX was observed. As depicted in the inset panel of Fig. 12, within somehow 5 h, the drug release was less than 10%.

Conclusion

A pH-responsive magnetic nanocomposite was successfully prepared by RAFT polymerization, and its structure and delivery application were studied. FESEM images for the Fe_3O_4/poly(SEMA-*co*-MMA) nanocomposite demonstrated the spherical shapes and average diameter of 30 ± 10 nm. The VSM analysis demonstrated a saturation magnetization of 13.25 $emug^{-1}$ for the Fe_3O_4/poly(SEMA-*co*-MMA)

nanocomposite. The dispersibility tests also exhibited that the synthesized Fe_3O_4/poly(SEMA-*co*-MMA) nanocomposite was stable more than five months at ambient condition in deionized water solvent. The pH sensitivity of nanocomposite was also represented by DLS. The DOX release behaviors of DOX-loaded Fe_3O_4/P(SEMA-co-MMA) nanocomposite were accelerated at pHs of 4 and 5.4 compared to 7.4 at 37 °C. The results exhibited that the DOX-loaded Fe_3O_4/poly(SEMA-*co*-MMA) nanocomposite could be considered as an superlative candidate for drug delivery.

Acknowledgements We express our gratitude to the Payame Noor University for supporting this project.

Funding This study was not funded.

Compliance with ethical standards

Conflict of Interest The authors declare that they have no conflict of interest.

References

1. Bhowmick A, Saha A, Pramanik N, Banerjee S, Das M, Kundu PP (2015) Novel magnetic antimicrobial nanocomposites forbone tissue engineering applications. RSC Adv 5:25437–25445
2. Massoumi B, Mousavi-Hamamlu SV, Ghamkhari A, Jaymand M (2017) A novel strategy for synthesis of polystyrene/Fe3O4 nanocomposite: RAFT polymerization, functionalization, and coordination techniques. Polym-Plast Technol Eng 56:873–882
3. Zhu L, Wang D, Wei X, Zhu X, Li J, Tu C, Su Y, Wu J, Zhu B, Yan D (2013) Multifunctional pH-sensitive superparamagnetic iron-oxide nanocomposites for targeted drug delivery and MR imaging. J Control Release 169:228–238
4. Wang W, Zhang Z (2007) Hydrothermal synthesis and characterization of carbohydrate microspheres coated with magnetic nanoparticles. J Dispers Sci Technol 28:557–561
5. Cheng R, Meng F, Deng C, Klok H-A, Zhong Z (2013) Dual and multi-stimuli responsive polymeric nanoparticles for programmedsite-specific drug delivery. Biomaterials 34:3647–3657
6. Hergt R, Dutz S, Muller R, Zeisberger M (2006) Magnetic particle hyperthermia: nanoparticle magnetism and materials development for cancertherapy. J Phys Condens Matter 18:S2919–S2934
7. Karumanchi RS, Doddamane SN, Sampangi C, Todd PW (2002) Field-assisted extraction of cells, particles and macromolecules. Trends Biotechnol 20:72–78
8. Jiang Y, Guo C, Xia H, Mahmood I, Liu C, Liu H (2009) Magnetic nanoparticles supported ionic liquids for lipase immobilization: Enzyme activity in catalyzing esterification. J Mol Catal B Enzym 58:103–109
9. Caoa J, Wanga Y, Yu J, Xiaa J, Zhanga C, Yina D, Hafeli UO (2004) Preparation and radiolabeling of surface-modifiedmagnetic nanoparticles with rhenium-188 formagnetic targeted radiotherapy. J Magn Magn Mater 277:165–174
10. Zhang X, Yang P, Dai Y, Ma P, Li X, Cheng Z, Hou Z, Kang X, Li C, Lin J (2013) Multifunctional up-converting nanocomposites with smart polymer brushes gated mesopores for cell imaging and thermo/pH dual-responsive drug controlled release. Adv Funct Mater 23:4067–4078
11. Oha JK, Park JM (2011) Iron oxide-based superparamagnetic polymeric nanomaterials: design, preparation, and biomedical application. Prog Polym Sci 36:168–189
12. Sivudu KS, Rhee KY (2009) Preparation and characterization of pH-responsive hydrogel magnetite nanocomposite. Colloids Surf A Physicochem Eng Asp 349:29–34
13. Lee JE, Lee DJ, Lee N, Kim B, Choi SH, Hyeon T (2011) Multifunctional mesoporous silica nanocomposite nanoparticles for pH controlled drug release and dual modal imaging. J Mater Chem 21:16869–16872
14. Poorgholy N, Massoumi B, Jaymand M (2017) A novel starch-based stimuli-responsive nanosystem for theranostic applications. Int J Biol Macromol 97:654–661
15. Pietsch C, Hoogenboom R, Schubert US (2010) PMMA based soluble polymeric temperature sensors based on UCST transition and solvatochromic dyes. Polym Chem 1:1005–1008
16. Chi W, Liu S, Yang J, Wang R, Ren H, Zhou H, Chenb J, Guo T (2014) Evaluation of the effects of amphiphilic oligomers in PEI based ternary complexes on the improvement of pDNA delivery. J Mater Chem B 2:5387–5396
17. Fran J, Lutz C (2006) Solution self-assembly of tailor-made macromolecular building blocks prepared by controlled radical polymerization techniques. Polym Int 55:979–993
18. Delaittre G, Save M, Gaborieau M, Castignolles P, Rieger J, Charleux B (2012) Synthesis by nitroxide-mediated aqueous dispersion polymerization, characterization, and physical core-crosslinking of pH- and thermoresponsive dynamic diblock copolymer micelles. Polym Chem 3:1526–1538
19. Beers KL, Boo S, Gaynor SG, Matyjaszewski K (1999) Atom transfer radical polymerization of 2-hydroxyethyl methacrylate. Macromolecules 32:5772–5776
20. Ahmed M, Narain R (2013) Progress of RAFT based polymers in gene delivery. Prog Polym Sci 38:767–790
21. Davaran S, Ghamkhari A, Alizadeh E, Massoumi B, Jaymand M (2017) Novel dual stimuli-responsive ABC triblock copolymer: RAFT synthesis, Schizophrenic" micellization and its performance as an anticancer drug delivery nanosystem J Colloid Interface Sci 488:282–293
22. Yang C, Guo W, Cui L, An N, Zhang T, Lin H, Qu F (2014) pH-Responsive magnetic core-shell nanocomposites for drug delivery. Langmuir 30:9819–9827
23. Bastakoti BP, Guragain S, Nakashima K, Yamauchi Y (2015) Stimuli-induced core–corona inversion of micelle of poly(acrylic acid)-block-poly(N-isopropylacrylamide) and its application in drug delivery. Macromol Chem Phys 216:287–291
24. Huang G, Zhang K-L, Chen S, Li S-H, Wang L-L, Wang L-P, Liu R, Gao J, Yang H-H (2017) Manganese-iron layered double hydroxide: a theranosticnanoplatform with pH-responsive MRI contrast enhancement and drug release. J Mater Chem B 5:3629–3633
25. Ghamkhari A, Massoumi B, Jaymand M (2017) Novel 'schizophrenic' diblock copolymer synthesized via RAFT polymerization: Poly(2-succinyloxyethyl methacrylate)-*b*-poly[(N-4-vinylbenzyl), N,N-diethylamine]. Des Monomers Polym 20:190–200
26. Ma WF, Wu KY, Tang J, Li D, Wei C, Guo J, Wang SL, Wang CC (2012) Magnetic drug carrier with a smart pH-responsive polymer network shell for controlled delivery of doxorubicin. J Mater Chem 22:15206–15214
27. Li PY, Lai PS, Hung WC, Syu WJ (2010) Poly(L-lactide)-vitamin E TPGS nanoparticles enhanced the cytotoxicity of doxorubicin in drug-resistant MCF-7 breast cancer cells. Biomacromolecules 11:2576–2582
28. Massoumi B, Ghamkhari A, Agbolaghi S (2017) Dual stimuli-responsive poly(succinyloxyethylmethacrylate-*b*-*N*-Isopropylacrylamide) block copolymers *as* nano-carriers and respective application in Doxorubicin delivery. Int J Polym Mater. https://doi.org/10.1080/00914037.2017.1300901

29. Salehi R, Rasouli S, Hamishehkar H (2015) Smart thermo/pH responsive magnetic nanogels for the simultaneous delivery of doxorubicin and methotrexate. Int J Pharm 487:274–284
30. Bol'bukha YN, Tertykha VA, Yurkovb GY, Ovchenkov EA (2011) Synthesis and properties of nanocomposites based on magnetite and biocompatible polymers. Russ J Appl Chem 84:847–853
31. Rahimi M, Shojaei S, Safa KD, Ghasemi Z, Salehi R, Yousefi B, Shafiei-Irannejad V (2017) Biocompatible magnetic tris(2-aminoethyl)amine functionalized nanocrystalline cellulose as a novel nanocarrier for anticancer drug delivery of methotrexate. New J Chem 41:2160–2168
32. Massoumi B, Poorgholy N, Jaymand M (2017) Multi-stimuli responsive polymeric nanosystems for theranostic applications. Int J Polym Mater 66:38–47
33. Shivakumar HG, Fathima SJ, Radha V, Khanum F (2016) pH and thermosensitive 5-fluorouracil loaded poly (NIPAM-co-AAc) nanogels for cancer therapy. RSC Adv 6:105495–105507
34. Bawa P, Pillay V, Choonara YE, du Toit LC (2009) Stimuli-responsive polymers and theirapplications in drug delivery. Biomed Mater 4:022001
35. Cheng R, Wang X, Chen W, Meng F, Deng C, Liuband H, Zhong Z (2012) Biodegradable poly(3-caprolactone)-g-poly(2-hydroxyethyl methacrylate)graft copolymer micelles as superior nano-carriers for "smart" doxorubicinrelease. J Mater Chem 22:11730–11738